Water–Rock Interaction, Wanty & Seal II (eds)
© 2004 Taylor & Francis Group, London, ISBN

Mineral dissolution at the granite–saprolite interface

H.L. Buss & S.L. Brantley
Department of Geosciences, The Pennsylvania State University, University Park, PA, USA

P.B. Sak
Department of Geology, Bucknell University, Lewisburg, PA, USA

A.F. White
US Geological Survey, Menlo Park, CA, USA

ABSTRACT: The Rio Icacos watershed in Puerto Rico's Luquillo Experimental Forest is located on the Tertiary Rio Blanco quartz diorite bedrock mantled by 200–800 cm of saprolite. Previous workers have documented large differences in mineralogy and chemistry between the bedrock and the overlying saprolite. Those studies have predominately focused on wholesale changes between the bedrock and the saprolite. Herein we present a detailed examination of the weathering across the bedrock-saprolite interface. At the study site, the bedrock weathers spheroidally, forming corestones surrounded by 20–60 cm of concentric layers of weathering rock. We are exploring the chemistry and mineralogy of this complex interface between the corestones and saprolite at the microscale using inductively coupled plasma-mass spectrometry (ICP-MS), optical microscopy, scanning electron microscopy (SEM), energy dispersive X-ray spectroscopy (EDS), and electron probe microanalysis (EPMA) to characterize the chemical and physical processes that propagate the weathering front. Preliminary results from EPMA and SEM indicate that weathering is localized in cracks and along the edges of the weathering rock layers. At the outer edge of the corestone and along cracks within the first spheroidal layer, both plagioclase and hornblende release Al in the presence of water and a hydrous aluminosilicate phase precipitates in the void space. ICP-MS results are used to calculate the open-system mass transport (loss or gain) of the elements with respect to the corestone, accounting for density differences across the sampled section. These calculations show that most of the spheroidal layers have a bulk chemistry similar to the corestone but slightly depleted in most elements, with the largest chemical differences in the layer adjacent to the saprolite. Across the interface zone, the average order of mobility of the cations is $Ca > P > Na > Si > Al > Fe > Mg \approx Mn > K > Ti$.

1 INTRODUCTION

Little is known about how cohesive bedrock dissolves and disaggregates into saprolite. The rate of advance of the bedrock-saprolite interface into the subsurface depends upon water permeation and mineral dissolution. To study these phenomena, we investigate granite weathering in the Luquillo Experimental Forest (LEF) of Puerto Rico. The Rio Icacos watershed in the LEF has the highest documented chemical weathering rate of granitic rocks in the world (White et al. 1998). The Guaba Ridge in the Rio Icacos watershed is composed of Tertiary age Rio Blanco quartz diorite bedrock capped with 200–800 cm of saprolite and topped by 50–100 cm of soil. Weathering of the bedrock to saprolite in the Rio Icacos watershed has been studied and the processes by which the plagioclase, biotite, and quartz weather have been established (Murphy et al. 1998; White et al. 1998; Schulz & White 1999; White et al. 2001; White 2002; Turner et al. 2003; Riebe et al. 2003). However, the processes controlling hornblende dissolution from the bedrock has yet to be systematically investigated. Hornblende is ubiquitous in the bedrock but absent in the saprolite. Previous mineral weathering studies at this site have either not reported (Murphy et al. 1998; White et al. 1998; Schulz & White 1999) or characterized (Turner et al. 2003) partially weathered hornblende. The absence of hornblende within the saprolite suggests that hornblende must weather completely at the bedrock-saprolite interface. However, the interface is not

simple, but is comprised of about 20–60 cm of spheroidal weathering layers surrounding corestones. Each of these closely spaced layers of intact, but weathered, bedrock is about 2–6 cm thick.

Corestones are residual bedrock that is weathered in place into boulders (Linton 1955; Ollier 1971). *Exfoliation* describes the formation of sheets of rock by any weathering process although the term is more commonly used for large scale sheeting formed by tectonic forces, unloading, or confining stress. *Spheroidal weathering* is a specific type of exfoliation in which corestones are surrounded by concentric layers of weathering rock (Ollier 1971). Spheroidal weathering is synonymous with *concentric* or *onion-skin weathering* although Twidale (1968) differentiated thin sheeting as spheroidal and thick sheeting as onion-skin weathering. The sheets formed by spheroidal processes are variously called sheets, layers, shells, plates, scales, or rindlets (Bisdom 1967; Ollier 1971; Fritz & Ragland 1980). The term *rindlets* was used by Turner et al. (2003) to describe layers of weathering rock within the Rio Icacos saprolite. Although those rindlets are related to the present study, they are not part of the corestone-saprolite interface, but are isolated within the saprolite. Therefore, we use different terminology here to identify the spheroidal or onion-skin layers surrounding the corestones as distinct from the rindlets of Turner et al. (2003).

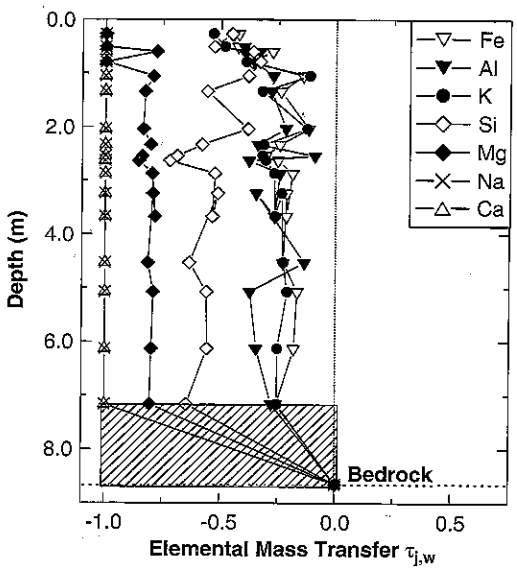

Figure 1. Elemental mass transfer with depth in the Rio Icacos saprolite adapted from White et al. (1998). The shaded region indicates the approximate zone sampled for the current study.

The abrupt changes in mineralogy and chemistry between the bedrock and saprolite reported in previous work at the Rio Icacos site span the onion-skin interface zone (Fig. 1). Herein, we present detailed chemical and mineralogical microanalyses of the onion-skin weathering zone using ICP-MS, optical microscopy, SEM, EDS, and EPMA. Our approach is to analyze chemical weathering at the site in a manner similar to previous workers (White et al. 1998; White et al. 2001; White 2002; Riebe et al. 2003; Turner et al. 2003) but at a finer scale (Fig. 1). In this way we plan to examine processes by which hornblende weathers and by which the complex onion-skin weathering front forms and propagates.

2 METHODS

A suite of 10 samples was collected at a road cut in the LEF by carefully removing a complete 49 cm continuous section of onion-skin layers and part of the adjacent corestone (Fig. 2). The 200 cm of overlying saprolite was sampled every 10 cm from the top onion-skin layer up to the ground surface.

Thin-sections were prepared from each sample set, straddling the edges of the weathering layers. Minerals within the thin sections were identified using optical microscopy and EPMA (Cameca SX-50). Backscattered electron maps of the thin-sections were made on an FEI Quanta 400 SEM.

Bulk elemental analysis of both major and minor elements was performed by ICP-MS of pulverized and sieved samples from each of the weathering layers. Mass transfer (loss or gain from the corestone)

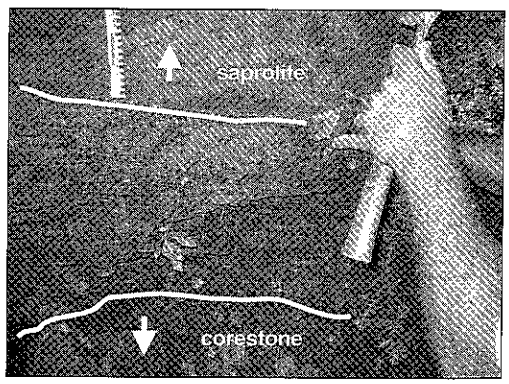

Figure 2. A continuous 49 cm section of the onion-skin layers (between the white lines) at the saprolite-corestone interface was carefully sampled. The upper portion of the corestone and every 10 cm of the entire 2 m of overlying saprolite were also sampled. Arm of A.F. White shown for scale. A schematic diagram of this sampled section is shown in Figure 4.

of individual elements relative to Ti was calculated for each section of weathered rock layers (Brimhall & Dietrich 1987). Mass transport in an open-system can be quantified when the parent material is homogenous (Rio Blanco quartz diorite), of uniform age (Tertiary), and contains an inert component (Ti) present in both the parent and product material (Chadwick et al. 1990). The immobility of Ti in the Rio Icacos watershed was determined by White et al. (1998) and confirmed by our calculations of volumetric strain with respect to Ti. Mass transfer (gain or loss) of an element j from a sample i, relative to the parent rock is calculated as:

$$\tau_{i,j} = \left(\frac{\rho_w C_{j,w}}{\rho_p C_{j,p}}\right)(\varepsilon_{Ti,w} + 1) - 1 \qquad (1)$$

where, $\varepsilon_{Ti,w}$ is the volumetric strain for Ti, ρ_w is dry bulk density of the weathered layer, ρ_p is dry bulk density of the parent rock (corestone), $c_{j,w}$ is mass concentration of element i in the weathered layer, and $c_{j,p}$ is mass concentration of element i in the corestone. The more negative the value of $\tau_{i,j}$ the more mobile the element, such that if $\tau_{i,j} = -1$, element j is entirely lost. If $\tau_{i,j} > 0$, a net gain of element j relative to the corestone is indicated.

3 RESULTS AND DISCUSSION

In thin-section, no porosity is evident in the corestone (Sample 10), whereas, the first onion-skin layer (Sample 8) above the corestone contains several channels (Figs. 3 & 4). The channels cut through all minerals without preference; therefore, control of channel formation does not appear to be chemical or mineralogical but rather physical. Minerals along channels are broken up by multiple cracks and have more void space in and around them (Fig. 5), suggesting that once channels exist, they provide wetted surface area that allows water to penetrate and weather minerals further into the rock. In this manner, a positive feedback loop is established in which void space permits water infiltration, which weathers minerals to create more void space.

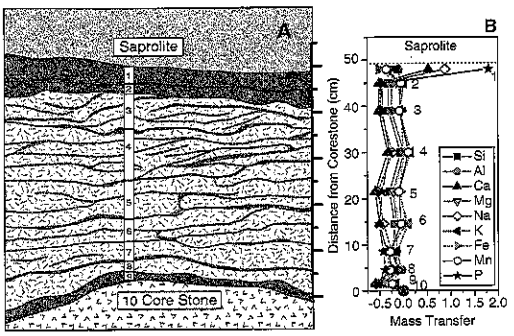

Figure 4. (A) Schematic drawing of sampled section (also shown in Fig. 2). Dark patterned areas are more friable than the light patterned onion-skin layers, but are not entirely weathered to saprolite. The onion-skin layers in the mid-section of the diagram are weathered but cohesive rock. Numbers correspond to locations of samples analyzed by ICP-MS from which loss or gain of elements from the corestone (mass transfer) was calculated shown as in (B) at the same scale as (A).

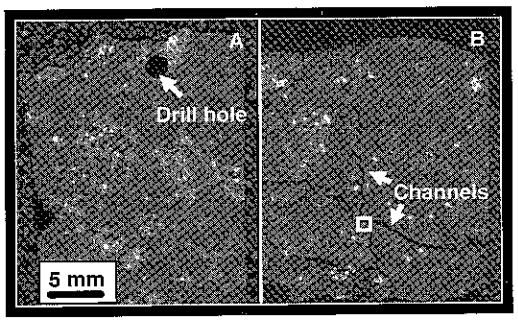

Figure 3. Backscattered electron maps of thin-sections. The top edge of the thin-section in (A) is the edge of the corestone nearest the ground surface (Sample 10, see Fig. 4). No secondary porosity is evident in the corestone. The thin-section in (B) entirely spans the first onion-skin layer above the corestone (Sample 8, see Fig. 4) and is oriented such that the top is nearest the ground surface and the bottom is towards the corestone. Several channels cross-cut this onion-skin layer. The box indicates the area shown in Figure 5.

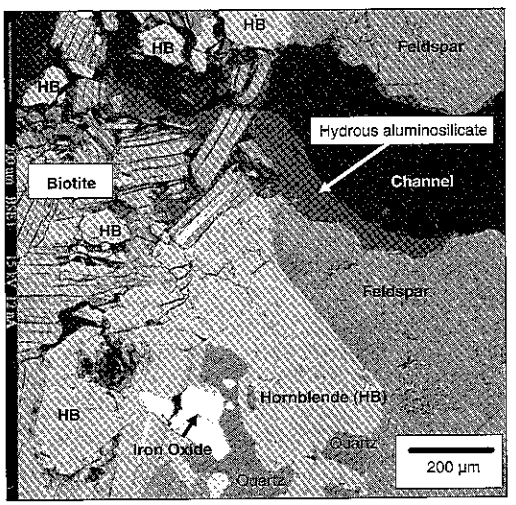

Figure 5. Backscattered electron image of a region surrounding one of the channels seen in Figure 3B.

Lining the channels of sample 8, EPMA revealed a hydrous aluminosilicate material (kaolinite?) not present elsewhere in the samples (Fig. 5). Clay minerals are found only near void spaces such as channels, cracks, or edges of the rock layers. In Sample 8, plagioclase crystals adjacent to clays or void space have less Ca and Al relative to Si than plagioclase not bordering clays or void space, as analyzed by EPMA. Similarly, hornblende crystals adjacent to void space or clays have slightly less Na and Al relative to Si than hornblende not in contact with void space or clays. Evidently the channels allow fluids to infiltrate the rock and are the focus of incongruent dissolution and precipitation of secondary phases. It remains unclear which phase weathers first.

The Al-rich material lining the channels may be precipitated from the Al released from weathered plagioclase and hornblende. Average atomic ratios of Al/Si in unweathered minerals (0.58, 0.16) are larger than the Al/Si in weathered minerals (0.49, 0.12) for plagioclase and hornblende, respectively. The higher Al content and abundance (~56 vs. ~6 wt.% of the bedrock mineralogy; White et al. 1998) of plagioclase compared to hornblende indicate that plagioclase is therefore likely the primary contributor to the Al in the precipitate within the channels.

"Micro-cracks" have been related to spheroidal weathering in granites by Bisdom (1967) who suggested that chemical and physical processes widen pre-existing fractures and cleavages and form new cracks along zones of weakness. Unlike that study, our samples contain no pre-existing fractures or cleavages and weathering-induced cracks appear to cut through crystals indiscriminately (Figs. 3 & 5).

Bisdom (1967) suggests that swelling and contraction creates and widens micro-cracks. Also, expansion of biotite to hydrobiotite or clays can fracture granite to form grus (Eggler et al. 1969; Isherwood & Street 1976) and has been implicated in spheroidal weathering (Chapman & Greenfield 1949). However, this mechanism has been disputed because spheroidal weathering usually occurs isovolumetrically and often at depths where expansion is improbable due to overlying rock (Ollier 1971).

Ollier (1971) also states that crack formation is likely the first step in the spheroidal weathering process and mentions the role of infiltrating water in transporting material to maintain constant volume during weathering. This is consistent with the isovolumetric weathering at our site indicated by White et al. (1998) and our mass transfer calculations.

Mass transfer calculations show that the average order of mobility of cations in the interface zone relative to the corestone is $Ca > P > Na > Si > Al > Fe > Mg \approx Mn > K > Ti \approx 0$. This is different from what is seen in the saprolite $Na \approx Ca > Mg > Si > K > Al > Fe > Ti \approx 0$ (White et al. 1998). Mass transfer calculations also show that most of the onion-skin layers are only slightly depleted in most elements relative to the corestone (Fig. 4). The largest bulk chemical differences relative to the corestone are found in the 3 cm thick layer (Sample 1) adjacent to the saprolite. This friable, highly weathered layer is very different in texture from the relatively intact, rocky onion-skin layers below. This boundary layer has a net gain of P, Ca, and Na, the elements that are most depleted in the rocky layers below (Fig. 4). The large differences observed in this 3 cm layer indicate that the boundary between the saprolite and bedrock chemistry may be significantly more abrupt than the 150–200 cm transition zone recognized by others (Fig. 1; White et al. 1998; Riebe et al. 2003).

4 CONCLUSIONS

The spheroidal weathering zone between the saprolite and corestones in the Rio Icacos watershed is physically and chemically complex. Preliminary results suggest initial physical control of weathering exhibited by crack formation in the layers nearest the corestone and large chemical changes in the layers adjacent to the saprolite. These results imply that weathering starts locally near the corestone and intensifies at the outer edges of the spheroidal weathering zone. Further analyses of the weathering layers, corestones, and saprolite using EPMA, ICP-MS, XPS, SEM, and EDS are underway and will be presented. Questions remain about the relative order and rates of hornblende and plagioclase weathering, weathering mechanisms, and controls on crack formation. We seek to answer these questions and to explain the processes that govern the character and propagation of the weathering front via detailed investigations of the interface between the highly weathered saprolite and the unweathered bedrock.

ACKNOWLEDGEMENTS

We thank J. Troester and D. Mericle for field support, M. Angelone for EPMA assistance. Funding provided by NSF-IGERT grant DGE-9972759.

REFERENCES

Bisdom, E.B.A. 1967. The role of micro-crack systems in the spheroidal weathering of an intrusive granite in Galicia (NW Spain). *Geologie en Mijnbouw* 46: 333–340.

Brimhall, G.H. & Dietrich, W. E. 1987. Constitutive mass balance relations between chemical composition, volume, density, porosity, and strain in metasomatic

hydrochemical systems. *Geochim. Cosmochim. Acta* 51: 567–587.

Chadwick, O.A., Brimhall, G.H. & Hendricks, D.M. 1990. From black box to a grey box: a mass balance interpretation of pedogenesis. *Geomorphology* 3: 369–390.

Chapman, R.W. & Greenfield, M.A. 1949. Spheroidal weathering of igneous rocks. *Am. J. Sci.* 247: 407–429.

Eggler, D.H., Larson, E.E. & Bradley, W.C. 1969. Granites, grusses, and the Sherman erosion surface, southern Laramie Range, Colorado-Wyoming. *Am. J. Sci.* 267: 510–522.

Fritz, S.J. & Ragland, P.C. 1980. Weathering rinds developed on plutonic igneous rocks in the North Carolina piedmont. *Am. J. Sci.* 280: 546–559.

Isherwood, D. & Street, A. 1976. Biotite-induced grussification of the Boulder Creek Granodiorite, Boulder County, Colorado. *Geol. Soc. Am. Bull.* 87: 366–370.

Linton, D.L. 1955. The problem of tors. *Geog. J.*121 470–487.

Murphy, S.F., Brantley, S.L., Blum, A.E., White, A.F. & Dong, H. 1998. Chemical weathering in a tropical watershed, Luquillo Mountains, Puerto Rico: II. Rate and mechanism of biotite weathering. *Geochim. Cosmochim. Acta* 62: 227–243.

Ollier, C.D. 1971. Causes of spheroidal weathering. *Earth-Sci. Rev.*7: 127–141.

Riebe, C.S., Kirchner, J.W. & Finkel, R.C. 2003. Long-term rates of chemical weathering and physical erosion from cosmogenic nuclides and geochemical mass balance. *Geochim. Cosmochim. Acta* 67(22): 4411–4427.

Schulz, M.S. & White, A.F. 1999. Chemical weathering in a tropical watershed, Luquillo Mountains, Puerto Rico: III. Quartz dissolution rates. *Geochim. Cosmochim. Acta* 63: 337–350.

Turner, B.F., Stallard, R.F. & Brantley, S.L. 2003. Investigation of in situ weathering of quartz diorite bedrock in the Rio Icacos basin, Luquillo Experimental Forest, Puerto Rico. *Chem. Geol.* 202: 313–341.

Twidale, C.R. 1968. *Geomorphology, with special reference to Australia.* Melbourne: Nelson.

White, A.F., Blum, A.E., Schulz, M.S., Vivit, D.V., Stonestrom, D. A., Larsen, M., Murphy, S. F. & Eberl, D. 1998. Chemical weathering in a tropical watershed, Luquillo Mountains, Puerto Rico: I. Long-term versus short-term weathering fluxes. *Geochim. Cosmochim. Acta* 62: 209–226.

White, A.F., Bullen, T.D., Schulz, M.S., Blum, A.E., Huntington, T.G. & Peters, N.E. 2001. Differential rates of feldspar weathering in granitic regoliths. *Geochim. Cosmochim. Acta* 65: 847–869.

White, A.F. 2002. Determining mineral weathering rates based on solid and solute weathering gradients and velocities: application to biotite weathering in saprolites. *Chem. Geol.*190: 69–89.